

# A new interpretation of the remarkable X-ray spectrum of the symbiotic star CH Cyg

Peter J. Wheatley<sup>1\*</sup> and Timothy R. Kallman<sup>2</sup>

<sup>1</sup> *Department of Physics, University of Warwick, Coventry CV4 7AL, UK*

<sup>2</sup> *Laboratory for High-Energy Astrophysics, NASA Goddard Space Flight Center, Code 662, Greenbelt, MD 20771, USA*

## ABSTRACT

We have reanalysed the *ASCA* X-ray spectrum of the bright symbiotic star CH Cyg, which exhibits apparently distinct hard and soft X-ray components. Our analysis demonstrates that the soft X-ray emission can be interpreted as scattering of the hard X-ray component in a photo-ionised medium surrounding the white dwarf. This is in contrast to previous analyses in which the soft X-ray emission was fitted separately and assumed to arise independently of the hard X-ray component. We note the striking similarity between the X-ray spectra of CH Cyg and Seyfert 2 galaxies, which are also believed to exhibit scattering in a photo-ionised medium.

**Key words:** accretion, accretion discs – binaries: symbiotic – stars: individual: CH Cyg – white dwarfs – stars: winds, outflows – X-rays: binaries

## 1 INTRODUCTION

Symbiotic systems contain a red giant star but also exhibit high-ionisation features in optical/ultraviolet spectra. In most cases it is believed that a white dwarf companion is accreting from the wind of the giant.

Symbiotic stars tend also to be X-ray sources and Muerset et al. (1997) used *ROSAT* spectra to separate their X-ray emission into three distinct classes:  $\alpha$ ) supersoft emission (below 0.4 keV),  $\beta$ ) emission with a characteristic temperature of a few  $10^6$  K (peaking at  $\sim 0.8$  keV), and  $\gamma$ ) harder X-ray emission. These classes were interpreted as arising from:  $\alpha$ ) the photosphere of a hot white dwarf,  $\beta$ ) the collision of the wind of the giant with a high-velocity wind from the hot companion,  $\gamma$ ) a possible signature of a neutron star companion. One system, CH Cyg, was classed as exhibiting both a  $\beta$  component and a “residual  $\gamma$  component”.

Ezuka et al. (1998) observed CH Cyg with *ASCA*, which was sensitive to harder X-rays than was *ROSAT* (hard limits of 10 keV and 2.5 keV respectively). They found that the X-ray spectrum of CH Cyg is made up of apparently distinct hard and soft X-ray components. The soft component peaks at 0.8 keV and the hard component at 5 keV (see Fig. 1). Ezuka et al. (1998) interpreted the hard component as heavily-absorbed optically-thin thermal emission of material being accreted by the white dwarf. In common with previous authors (Leahy & Volk 1995; Muerset et al. 1997) they fitted the soft emission as a distinct optically-thin emission component. This was interpreted as either coronal emission from the giant star or shock heating in the radio/X-ray

jets of CH Cyg. Leahy & Volk (1995) and Muerset et al. (1997) both interpret the soft component as the result of shock heating in the collision of stellar winds from the giant and white dwarf.

Wheatley et al. (2003) reported a similar two-component spectrum in another symbiotic star, 4 Draconis. In this case the X-ray spectrum was seen to change between the two-component form and a single-component form. Wheatley et al. (2003) interpreted both spectra as representing emission *only* from an accreting white dwarf, but with a varying amount of partially-ionised absorption. Ionisation of the absorbing material removes absorption edges entirely from lighter elements (e.g. H, He), and shifts absorption edges of heavier elements to higher energies (e.g. O), allowing soft photons to leak through.

In this paper we consider whether similar models can account for the apparent two-component nature of the *ASCA* spectrum of CH Cyg. In doing so we draw attention to the striking similarity between the X-ray spectra of CH Cyg and Seyfert 2 galaxies.

## 2 OBSERVATIONS

CH Cyg was observed using the *ASCA* X-ray observatory (Tanaka et al. 1994) on 1994 October 19. *ASCA* carried four X-ray telescopes, of which two were equipped with CCD detectors (SIS0 and SIS1) and two with proportional counter detectors (GIS2 and GIS3). The SIS detectors had higher spectral resolution and better soft X-ray sensitivity, and in this paper we have limited our analysis to data from the SIS0 detector which also had the highest count rate. We have used

\* E-mail: p.j.wheatley@warwick.ac.uk

**Table 1.** Log of the *ASCA* SIS0 observations presented in this paper.

Target	seq. no.	Date	Exposure	Count rate
CH Cyg	42020000	1994-10-19	19.2 ks	$0.516 \text{ s}^{-1}$
NGC 4507	71029000	1994-02-12	28.3 ks	$0.126 \text{ s}^{-1}$
NGC 4388	73073000	1995-06-21	31.5 ks	$0.032 \text{ s}^{-1}$
NGC 7582	74026000	1996-11-21	39.7 ks	$0.011 \text{ s}^{-1}$

the standard screened data as extracted from the Leicester Database and Archive Service (LEDAS) at the University of Leicester. This yields an exposure time of 19.2 ks in the SIS0 instrument.

Data were reduced using *FTOOLS* software and standard techniques as described in the *ASCA* Data Reduction Guide<sup>1</sup>. The SIS0 source spectrum was extracted from a circular region of radius 4 arcmin, and the background was estimated from most of the remainder of the CCD. The mean background-subtracted count rate was  $0.516 \pm 0.006 \text{ s}^{-1}$ , yielding  $9890 \pm 120$  source counts. A log of observations is presented in Table 1.

### 3 SPECTRAL ANALYSIS

#### 3.1 Two emission components?

The SIS0 spectrum of CH Cyg is presented in Fig. 1. The two X-ray components discussed by Ezuka et al. (1998) are clearly visible either side of a minimum at 2 keV. Ezuka et al. (1998) fitted the spectrum with a complex multi-component model consisting of three separate plasma emission components (two for the soft emission and one for the hard emission) and three separate absorption components (one for the soft emission and two for the hard emission).

The solid line in Fig. 1 shows the results of a fit to the spectrum only above 2 keV. We used the *mekal* optically-thin thermal plasma model (Mewe et al. 1985, 1986; Kaastra 1992; Liedahl et al. 1995) absorbed by a neutral cosmic-abundance absorber. The best-fitting *mekal* temperature was 7.7 keV (characteristic of accreting white dwarfs) and the absorber column density was  $1.6 \times 10^{23} \text{ cm}^{-2}$ . As noted by Ezuka et al. (1998), this simple absorption model does not result in a good fit to the hard component (we found a reduced  $\chi^2$  of 1.9 with 282 degrees of freedom). This motivated Ezuka et al. (1998) to add a second, complex absorption component to their hard X-ray model (they used a partial-covering model). They did not, however, consider the possibility that the soft component itself could arise as a consequence of photons leaking through or around this complex absorber. The upper line in Fig. 1 shows the unabsorbed model spectrum. It can be seen that the implied soft X-ray flux from the hard component exceeds the detected flux by an order of magnitude. Even a small soft X-ray leak would easily account for the measured soft X-ray emission, avoiding the need for a second emission component.

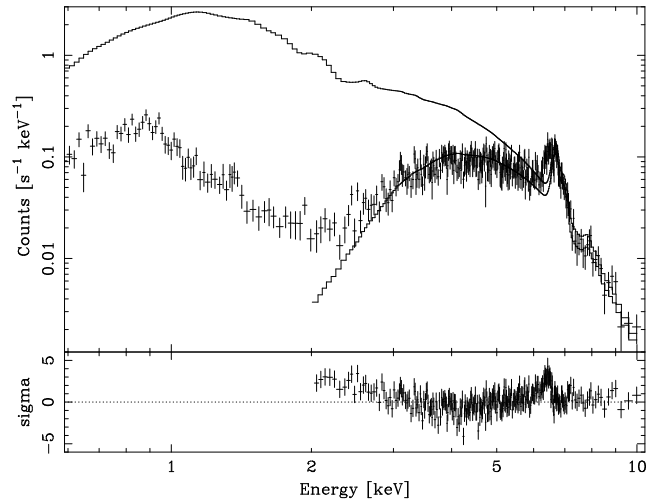


**Figure 1.** *ASCA* SIS0 spectrum of CH Cyg. The solid line running through the data points represents a simple fit to the spectrum above 2 keV (see text). The lower panel shows the residuals to the fit normalised by the error on each data point. The upper line in the top panel shows the unabsorbed model.

#### 3.2 A photo-ionised absorber?

Wheatley et al. (2003) successfully fitted the two-component X-ray spectrum of the symbiotic star 4 Draconis with a single emission component modified by a photo-ionised absorber. Ionisation of the absorbing medium removes absorption edges entirely from lighter elements (e.g. H, He) and shifts absorption edges of heavier elements to higher energies (e.g. O). The result is that soft X-rays leak through the absorber, giving rise to what can appear to be a separate emission component. In this section we investigate whether this same model might explain the two-component X-ray spectrum of CH Cyg.

In order to consider the possible effects of ionisation of the absorbing medium in CH Cyg we employed the *absori* model in *XSPEC* (Done et al. 1992; Zdziarski et al. 1995). This is a simple single-zone photo-ionisation model which assumes a power-law input spectrum. For this paper we modified the *absori* source code to use a bremsstrahlung spectrum as the ionising source, and we fixed the bremsstrahlung temperature to the *mekal* temperature of the hard component. The other parameters of the *absori* model are the column density,  $N_{\text{H}}$ , the temperature of the absorber,  $T_{\text{abs}}$ , and the ionisation parameter  $\xi = L/nR^2$ , where  $L$  is the integrated source luminosity between 5 eV and 300 keV,  $n$  is the density of the material, and  $R$  is the distance of the material from the illuminating source. In addition to the *absori* model we included a neutral absorption component to account for interstellar absorption.

Fitting with the *absori* model we found we needed high values of  $\xi$  ( $\sim 10^2 - 10^3$ ) in order to allow the soft X-ray leak to extend as hard as 2 keV. In contrast, the X-ray minimum between the two components occurred at around 1 keV in 4 Draconis, and Wheatley et al. (2003) found acceptable fits with  $\xi \sim 6$ .

The best fit with the *absori* model is plotted in Fig. 2 together with the model spectrum. It can be seen that the ionised absorber results in a better fit to the hard X-ray

<sup>1</sup> <http://heasarc.gsfc.nasa.gov/docs/asca/abc/abc.html>

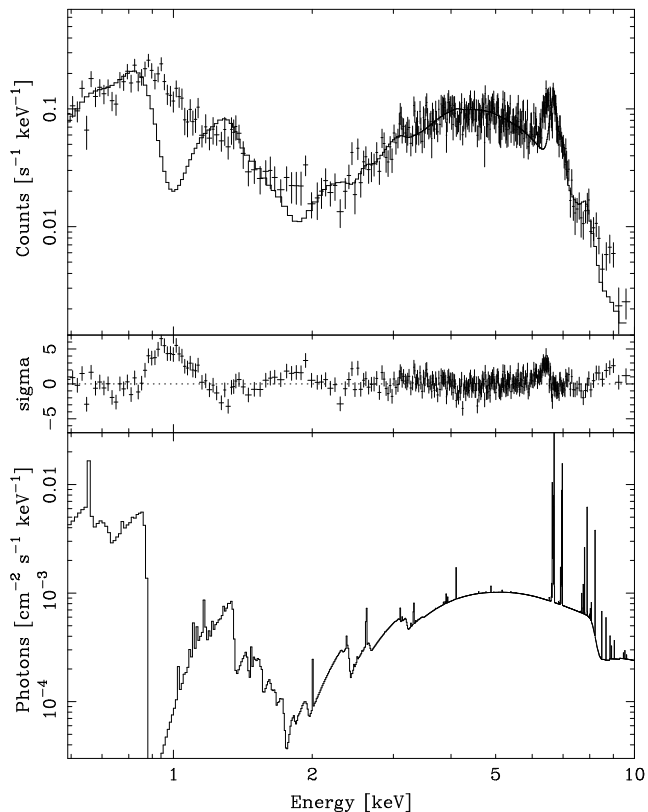


**Figure 2.** *ASCA* SIS0 spectrum of CH Cyg fitted with the *absori* ionised absorber model (top panel). The middle panel shows the residuals to the fit normalised by the error on each data point. The bottom panel shows the model spectrum.

emission between 2–5 keV than did the neutral absorber (Fig. 1). It also allows a sufficiently strong soft-X-ray leak to account reasonably well for the soft X-ray emission (although the fit is not statistically acceptable with a reduced  $\chi^2$  of 2.3 with 348 degrees of freedom). The best-fitting column density for the ionised absorber is  $N_{\text{H}} = 6.2 \times 10^{23} \text{ cm}^{-2}$ . The ionisation parameter was found to be anti-correlated with the temperature of the absorber, and equally good fits were found for  $\xi$  in the range 55–1000 (for  $T_{\text{abs}} = 10^6 - 10^4 \text{ K}$ ). The best-fitting *mekal* temperature was 7.1 keV and the neutral absorber had a column density of  $N_{\text{H}} = 2.2 \times 10^{21} \text{ cm}^{-2}$ .

Inspection of Fig. 2 shows that the strongest residuals occur at 0.9–1.0 keV, coincident with the strong OVIII K-shell edge in the *absori* model. Residuals are also apparent around 6.4 keV, the energy of the  $K_{\alpha}$  line of neutral iron.

Adding a narrow emission line fixed at 6.4 keV entirely removed the residuals at this energy and resulted in an improvement in reduced  $\chi^2$  to 1.94 (with 347 degrees of freedom). The line has an equivalent width of 220 eV, which is high for X-ray reflection from a cold slab such as the white dwarf surface (George & Fabian 1991). This indicates either partial ionisation of the reflecting medium or fluorescence from an additional location, perhaps an accretion disc and/or the wind of the red giant.

Removing the residuals in the 1 keV region is more difficult. Adding a narrow line also in the 1 keV region resulted in a considerable improvement in reduced  $\chi^2$  to 1.22 (with

345 degrees of freedom) with a best-fitting line energy of 0.95 keV. This line might represent recombination emission from oxygen, and indeed the fit statistic was further improved to 1.12 (345 d.o.f.) by replacing the narrow line with a radiative recombination continuum (RRC) with edge energy fixed at the OVIII K-shell energy (0.8714 keV). However, this fit relies on a high electron temperature (0.1 keV) to make the RRC sufficiently broad to cancel out the OVIII absorption edge. The perfect cancelling of these two features leads us to believe that neither are really present in the spectrum of CH Cyg.

### 3.2.1 Fluxes

The absorbed 0.6–10 keV flux of the best fit to the ionised absorber model was  $6.3 \times 10^{-11} \text{ erg cm}^{-2} \text{ s}^{-1}$  and the implied unabsorbed flux of the *mekal* model was  $2.0 \times 10^{-10} \text{ erg cm}^{-2} \text{ s}^{-1}$  corresponding to a bolometric luminosity of  $3 \times 10^{33} \text{ erg s}^{-1}$  at a distance of  $270 \pm 65 \text{ pc}$  (Viotti et al. 1997; Perryman et al. 1997). This corresponds to an accretion rate onto a white dwarf of around  $3 \times 10^{16} \text{ g s}^{-1}$  or  $5 \times 10^{-10} M_{\odot} \text{ yr}^{-1}$  (by considering the gravitational potential energy of material falling from infinity). This is a fairly robust estimate since it depends mainly on the temperature and normalisation of the *mekal* component. It does not rely on the ionised absorber interpretation.

### 3.2.2 Implied geometry

As stated above, the ionisation parameter is defined as  $\xi = L/nR^2$ . The column density is defined as  $N_{\text{H}} = nl$  where  $l$  is the path length through the absorber. The ionisation parameter can be written, therefore, also as  $\xi = Ll/N_{\text{H}}R^2$ . The path length through the absorber ( $l$ ) cannot be much larger than the distance of the absorber from the ionising source ( $R$ ), and so there is a maximum allowed distance of the absorber from the ionising source is given by  $R_{\text{max}} \sim L/N_{\text{H}}\xi$ . Taking the best fitting values for  $L$  and  $N_{\text{H}}$  and the allowed range of  $\xi$ , we find  $R_{\text{max}} \sim 5 \times 10^6 - 9 \times 10^7 \text{ cm}$  which is much smaller than the size of a white dwarf (typically  $\sim 7 \times 10^8 \text{ cm}$ ). Even allowing for extra X-ray luminosity that might be hidden by the absorber, an ionised absorber in CH Cyg would have to be located very close to the white dwarf.

## 3.3 A photo-ionised scattering medium?

As well as soft X-rays leaking *through* the absorber, it is also possible for soft X-rays to leak *around* the absorber. This is possible if the absorber is not isotropically distributed around the white dwarf and instead absorbs preferentially along our line of sight. Soft photons emitted in our direction would then be absorbed, but soft photons emitted in other directions would escape further from the white dwarf where they could be scattered into our line of sight in a lower-density photo-ionised medium.

This arrangement is essentially the same as is believed to exist in the nuclei of Seyfert 2 galaxies, where the anisotropic absorption is attributed to a highly inclined accretion disc or molecular torus. The *ASCA* spectra of Seyfert

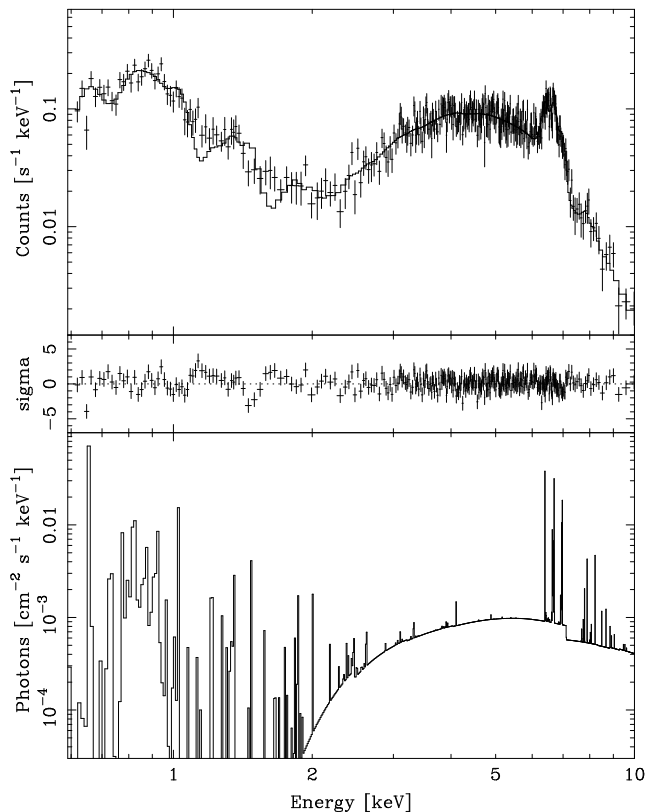


**Figure 3.** ASCA SIS0 spectrum of CH Cyg fitted with xSTAR photo-ionised scattering model (top panel). The middle panel shows the residuals to the fit normalised by the error on each data point. The bottom panel shows the model spectrum.

2 galaxies are actually remarkably similar to the spectrum of CH Cyg, and we discuss this further in Sect. 4.

In order to consider the possible effects of photo-ionised scattering in CH Cyg we have calculated model grids using the xSTAR photo-ionisation code (Kallman & McCray 1982; Kallman & Bautista 2001; Turner et al. 1996). This code calculates the absorption and emission spectra of a spherical shell of material surrounding a source of ionising photons. We used the emission spectrum of a model grid covering an ionisation parameter ( $\xi$ ) range of  $10^{-4} - 10^4$  (same definition as the *absori* model above) and a column density range of  $10^{19} - 10^{23} \text{ cm}^{-2}$ . The ionising spectrum was chosen to be an 8 keV bremsstrahlung in order to match approximately the emission of the white dwarf in CH Cyg. This model grid (grid23scatt) is available from the xSTAR webpage<sup>2</sup>.

We fixed the normalisation of the scattered spectrum to that appropriate to the unabsorbed flux of the fitted *mekal* emission component (a value of  $4.1 \times 10^{-4}$ ). We replaced the ionised absorber model with a neutral absorber, but included a second partial-covering absorber in order to account for the complexity apparent in Fig. 1. We also included a narrow emission line fixed at 6.4 keV and a third neutral absorber representing interstellar absorption.

Fitting with this model we found that the photo-ionised scattering region readily reproduced the strength and overall

flux distribution of the soft component in CH Cyg. We also found a statistically acceptable fit, with a reduced  $\chi^2$  of 1.09 (338 d.o.f.). This best fit is plotted in Fig. 3.

The strongest residuals in our best-fit scattering model occur between 1–2 keV. This corresponds to the energies of strong line emission in the *mekal* model, mainly due to iron L-shell, that were not included in our bremsstrahlung ionising spectrum. This missing input flux may account for these residuals. Alternatively, we have found that relaxing the constraint on the value of the normalisation of the scattering component allows a better fit to this region. In effect this allows for extra ionising flux that is hidden by the main absorber, which is plausible because accretion by white dwarfs is known to result in emission at a wide range of temperatures (e.g. Baskill et al. 2005). Finally, these residuals can also be reduced by allowing the relative elemental abundances to vary in the xSTAR model. However, since individual emission features are not resolved, none of these possible explanations are unique, and we did not pursue them in detail. We were satisfied that the scattering model is capable of producing the strength and overall shape of the soft component in CH Cyg.

### 3.3.1 Fitted parameters

The fitted parameters of the scattering region were  $N_{\text{H}} = (5.5 \pm_{0.8}^{1.3}) \times 10^{20} \text{ cm}^{-2}$  and  $\xi = 760 \pm_{130}^{70}$ . The parameters for the *mekal* emission component were essentially unchanged, with  $kT = 8.3 \pm 0.4 \text{ keV}$  and an unabsorbed 0.6–10 keV flux of  $(2.29 \pm 0.15) \times 10^{-10} \text{ erg s}^{-1} \text{ cm}^{-2}$ . The column densities of the main absorber are  $(9.7 \pm 0.7) \times 10^{22} \text{ cm}^{-2}$  and  $(2.9 \pm 0.5) \times 10^{23} \text{ cm}^{-2}$ . The former was applied to all the flux from the hard component, the latter had a partial covering fraction of  $66 \pm 4$  per cent. The column density of the absorber applied to the whole spectrum (including the scattered emission) was  $(2.6 \pm 0.5) \times 10^{21} \text{ cm}^{-2}$ . The equivalent width of the 6.4 keV line was  $200 \pm 20 \text{ eV}$ . All errors represent 68 per cent confidence intervals and account only for statistical errors.

### 3.3.2 Implied geometry

In Sect. 3.2.2 we showed that our fits to the ionised absorber model placed tight constraints on the geometry of the absorber. Our scattering model relaxes these constraints because the absorption of the hard component is decoupled from the source of the soft component. Since the ionisation parameter of the absorber is consistent with zero, the absorber can be placed at any distance from the ionising source. However, the scattering model does require the absorption to be anisotropic around the white dwarf, and so the absorber is still likely to be closely associated with that object.

The scattering region, in contrast, does have a well defined ionisation parameter in our model, and so we can apply the same argument used in Sect. 3.2.2 to constrain its distance from the ionising source. In this case  $R_{\text{max}} \sim 7 \times 10^9 \text{ cm}$ , which is around an order of magnitude larger than the white dwarf.

<sup>2</sup> <http://heasarc.gsfc.nasa.gov/docs/software/xstar/xstar.html>

#### 4 DISCUSSION AND CONCLUSIONS

The spectral analysis of Sect. 3 shows that the soft X-ray component in CH Cyg can be interpreted as a reprocessing of the hard X-ray component. The X-ray spectrum is explained without the need for a second source of X-rays in the system, such as from colliding winds.

In Sect. 3.2 we investigated the ionised absorber model used by Wheatley et al. (2003) to explain the two-component X-ray spectrum of 4 Draconis. This model reproduced the strength of the observed soft component, but it predicted a strong OVIII absorption edge that is not detected. The required combination of high column density and high ionisation parameter also implied that the absorber must be much smaller than the white dwarf. Overall we do not regard this model as an adequate explanation of the soft X-ray component of CH Cyg.

In Sect. 3.3 we considered an alternative explanation for the soft X-ray component in CH Cyg: scattering of the hard component in a photo-ionised medium. In this interpretation the absorber is not isotropically distributed around the white dwarf and instead absorbs preferentially along our line of sight. Soft photons emitted in our direction are absorbed, but soft photons emitted in other directions escape further from the white dwarf where they can be scattered into our line of sight in a lower-density photo-ionised medium. This scattering model provided a much more satisfactory explanation for the soft component in CH Cyg. It readily reproduced the strength and shape of the soft component. It also implied a distance to the scattering region that is much larger than the white dwarf.

As noted in Sect. 3.3, the *ASCA* spectrum of CH Cyg bears a striking resemblance to those of Seyfert 2 active galaxies. Examples include NGC 4388, NGC 7582 and NGC 4507 (Iwasawa et al. 1997; Xue et al. 1998; Comastri et al. 1998). In Fig. 4 we plot the *ASCA* SIS0 spectra of these systems, together with the spectrum of CH Cyg. The Seyfert 2 spectra have been extracted using the same method as described for CH Cyg in Sect. 2, and details of the observations are given in Table 1.

In Seyfert 2 galaxies our line of sight to the central black hole is believed to pass through a highly inclined accretion disc, or molecular torus, that provides the strong X-ray absorption apparent in the *ASCA* spectra (in some systems this region is Compton thick and blocks even hard X-rays). Soft X-ray components very much like that of CH Cyg are also observed (Fig. 4), and this has generally been interpreted as scattering in photo-ionised cones above and below the accretion discs/tori. This interpretation was strengthened by the apparent detection of the same ionised material in absorption in Seyfert 1 galaxies. The geometry described here is illustrated by the schematic diagrams in Fig. 7 of Awaki (1997) and Fig. 6 of Kinkhabwala et al. (2002), and is essentially the same interpretation as we favour for CH Cyg. There has been some debate over whether the soft X-ray components of Seyfert 2 galaxies can instead be dominated by collisionally ionised gas, perhaps from shock heating in outflows from the central region or from nuclear star-forming regions (similar interpretations to those proposed by previous authors for CH Cyg). However, the scattering model has now been confirmed in the Seyfert galaxies Mrk 3 and NGC 1068 using high-resolution X-ray spectra from *Chan-*

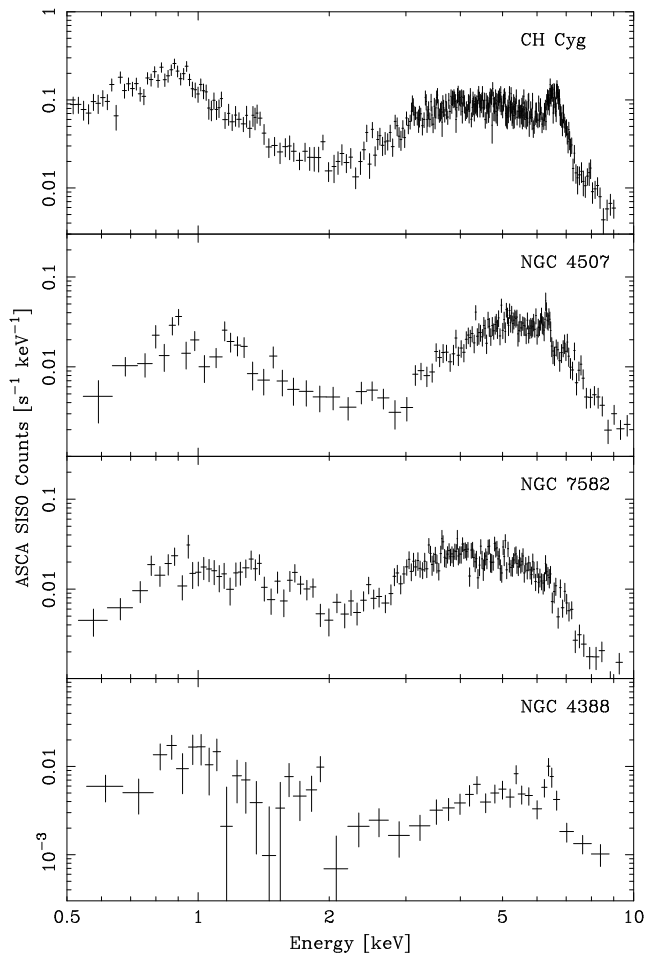


**Figure 4.** *ASCA* SIS0 spectrum of CH Cyg compared with those of three Seyfert 2 galaxies.

*dra* and *XMM-Newton* (Sako et al. 2000; Kinkhabwala et al. 2002; Brinkman et al. 2002).

The success of the scattering model in explaining the X-ray spectra of Seyfert 2 galaxies gives us increased confidence that this model is a likely explanation for the similar X-ray spectrum of CH Cyg. In Seyfert 2 galaxies the source of absorption is believed to be an edge-on accretion disc or torus. A highly inclined accretion disc may also account for the observed absorption in CH Cyg. The presence of a disc is supported by the detection of jets (Taylor et al. 1986; Galloway & Sokoloski 2004) and there is further evidence that CH Cyg may be viewed at high inclination (e.g. Skopal et al. 1996).

The scattering interpretation of the X-ray spectrum of CH Cyg is attractive because it requires only one source of X-rays: an accreting white dwarf. In contrast, Ezuka et al. (1998) invoke a second X-ray source, and still require a complex treatment of absorption and emission (three components of each). Several mechanisms have been invoked in order to explain this second source of X-rays, including colliding winds, jet shocks and coronal emission from the giant star (Leahy & Volk 1995; Muerstet et al. 1997; Ezuka et al. 1998). A consequence of our analysis is that these sources are no longer required to explain the X-ray spectrum of CH Cyg.

A definitive test of this model would be provided by high-resolution X-ray grating spectra of CH Cyg.

## ACKNOWLEDGEMENTS

We thank Koji Mukai, Simon Vaughan and Chris Done for useful discussions, and the Jenő Sokoloski for helpful comments on the original version of this paper. We also thank the referee, Jan-Uwe Ness, for helpful comments. Data used in this paper have been obtained from the Leicester Database and Archive Service (LEDAS) at the University of Leicester.

## REFERENCES

- Awaki H., 1997, in ASP Conf. Ser. 113: IAU Colloq. 159: Emission Lines in Active Galaxies: New Methods and Techniques ASCA Observations of Seyfert 2 Galaxies. pp 44–+
- Baskill D. S., Wheatley P. J., Osborne J. P., 2005, MNRAS, 357, 626
- Brinkman A. C., Kaastra J. S., van der Meer R. L. J., Kinkhabwala A., Behar E., Kahn S. M., Paerels F. B. S., Sako M., 2002, A&A, 396, 761
- Comastri A., Vignali C., Cappi M., Matt G., Audano R., Awaki H., Ueno S., 1998, MNRAS, 295, 443
- Done C., Mulchaey J. S., Mushotzky R. F., Arnaud K. A., 1992, ApJ, 395, 275
- Ezuka H., Ishida M., Makino F., 1998, ApJ, 499, 388
- Galloway D. K., Sokoloski J. L., 2004, ApJ, 613, L61
- George I. M., Fabian A. C., 1991, MNRAS, 249, 352
- Iwasawa K., Fabian A. C., Ueno S., Awaki H., Fukazawa Y., Matsushita K., Makishima K., 1997, MNRAS, 285, 683
- Kaastra J. S., 1992, Technical report, An X-Ray Spectral Code for Optically Thin Plasmas. SRON-Leiden
- Kallman T., Bautista M., 2001, ApJS, 133, 221
- Kallman T. R., McCray R., 1982, ApJS, 50, 263
- Kinkhabwala A., Sako M., Behar E., Kahn S. M., Paerels F., Brinkman A. C., Kaastra J. S., Gu M. F., Liedahl D. A., 2002, ApJ, 575, 732
- Leahy D. A., Volk K., 1995, ApJ, 440, 847
- Liedahl D. A., Osterheld A. L., Goldstein W. H., 1995, ApJ, 438, L115
- Mewe R., Gronenschild E. H. B. M., van den Oord G. H. J., 1985, A&AS, 62, 197
- Mewe R., Lemen J. R., van den Oord G. H. J., 1986, A&AS, 65, 511
- Muerset U., Wolff B., Jordan S., 1997, A&A, 319, 201
- Perryman M. A. C., et al., 1997, A&A, 323, L49
- Sako M., Kahn S. M., Paerels F., Liedahl D. A., 2000, ApJ, 543, L115
- Skopal A., Bode M. F., Lloyd H. M., Tamura S., 1996, A&A, 308, L9
- Tanaka Y., Inoue H., Holt S. S., 1994, PASJ, 46, L37
- Taylor A. R., Seaquist E. R., Mattei J. A., 1986, Nature, 319, 38
- Turner T. J., George I. M., Kallman T., Yaqoob T., Zycki P. T., 1996, ApJ, 472, 571
- Viotti R., Badiali M., Cardini D., Emanuele A., Iijima T., 1997, in ESA SP-402: Hipparcos - Venice '97 HIPPARCOS Astrometry and Radio Mapping of Peculiar Binary Systems. pp 405–408
- Wheatley P. J., Mukai K., de Martino D., 2003, MNRAS, 346, 855
- Xue S., Otani C., Mihara T., Cappi M., Matsuoka M., 1998, PASJ, 50, 519
- Zdziarski A. A., Johnson W. N., Done C., Smith D., McNaron-Brown K., 1995, ApJ, 438, L63